Gallium Nitride-on-Silicon Micromechanical Overtone Resonators and Filters

Azadeh Ansari[1], Vikrant J. Gokhale[1], Vikram A. Thakar[1], John Roberts[2], and Mina Rais-Zadeh[1]

[1]Department of Electrical Engineering & Computer Science, University of Michigan, Ann Arbor, MI 48109, USA
[2]Nitronex Corporation, Durham, North Carolina, USA
Phone: (734)764-4249, Fax: (734)763-9324, Email: azadans@umich.edu

Abstract

In this paper, for the first time, we report on high-performance GaN-on-silicon micromechanical resonators and filters. A GaN-on-silicon resonator is reported which exhibits a quality factor of 1850 at 802.5 MHz, resulting in an $f\times Q$ value twice the highest reported for GaN-based resonators to date. The effective coupling coefficient for the GaN resonator is extracted to be 1.7%, which is among the best reported in the literature.

Introduction

Gallium nitride (GaN) is a promising material for applications in high-power, high-temperature electronic devices, UV emitters, UV detectors and blue LEDs [1]. GaN-based electronics have attracted much attention in recent years. However, despite its many unique mechanical and acoustic properties, there has not been much research on GaN for MEMS applications. Our group has previously reported on the highest quality factor (Q) single crystalline GaN resonators with frequencies higher than 1 GHz [2], [3]. In this paper, for the first time, we report on high-performance GaN-on-silicon thin film piezoelectric on substrate (TPoS) resonators and filters (Fig. 1).

TPoS resonators [4] have been demonstrated in prior work using more conventional piezoelectric materials such as AlN [5], ZnO [6] and PZT [7]. In most of these implementations, the silicon layer dominates the stack structure and thus the resonance frequency and mode shape. Silicon with a higher energy density than the materials in question improves the Q when compared to the case of single material piezoelectric resonators. Furthermore, since silicon is a low-acoustic loss material, the thick silicon layer suppresses the acoustic non-linearity of the piezoelectric material, leading to a more linear and distortion-free performance at higher power levels. GaN is the prime candidate for TPoS structure as the acoustic velocity of GaN is very close to silicon, resulting in lower acoustic mismatch. The silicon layer in the GaN-on-silicon TPoS stack not only improves the acoustic properties of the resonator but can also be used as the bottom electrode, eliminating the need for bottom metallization. It is specifically difficult to embed a bottom metal layer in a GaN epi stack, as GaN cannot be epitaxially grown on any metal. Previous GaN resonator implementations have used backside sputtered metals [8], or two-degree electron gas (2DEG) as the bottom electrode [9]. In this work, we report on GaN TPoS resonators and filters which benefit from the silicon in the stack to achieve 100% improvement in $f\times Q$ values and better power handling when compared to single crystalline GaN resonators.

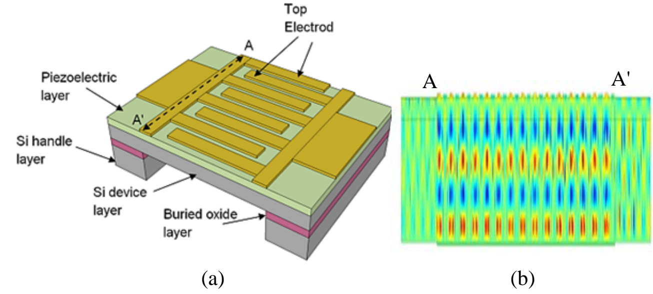

(a) (b)

Fig. 1. (a) A schematic view showing the TPoS filter configuration. (b) An exemplary 5th-order thickness resonance mode.

Fabrication Process

TPoS resonators and filters reported in this paper were all fabricated on the same silicon-on-insulator (SOI) substrate. The epitaxial GaN layer was grown on a 100 mm diameter SOI wafer in a custom-built, cold wall, rotating disc metalorganic chemical vapor deposition (MOCVD) reactor at nominal temperature of 1020 ºC. The SOI substrate consisted of a 2 μm thick buried silicon dioxide layer and a 10 μm thick p-type (0.001-0.01 Ω.cm) Si <111> device layer (miscut angle ±0.5˚). For the MOCVD growths, trimethylgallium (TMG) and trimethylaluminum (TMA) precursors were carried by Pd-diffused hydrogen, and ammonia (NH_3) was used as the N precursor. The full epitaxial stack consists of an AlN nucleation layer, two AlGaN layers, and a ~0.75 μm thick GaN buffer layer (Fig. 2(a)). The total thickness of the epi-layer is 1.43 μm.

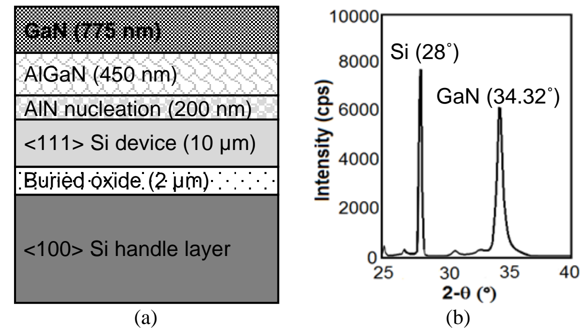

(a) (b)

Fig. 2. (a) GaN-on-SOI wafer stack and (b) XRD of the thin film GaN layer showing an FWHM of 0.535˚.

The advantage of growing GaN on SOI rather than on silicon is the lower built-in stress in the GaN film when grown on a

thinner silicon device layer which in turn results in a better quality thin film and fewer dislocations [10]. X-ray diffraction (XRD) measurements for the wafer show a Full Width at Half Maximum (FWHM) of 0.535º (Fig. 2(b)), indicating a high quality GaN-on-silicon film.

The fabrication process of GaN devices is shown in Fig. 3. It consists of five masks and starts with deposition of 50 nm thick plasma enhanced chemical vapor deposited (PECVD) silicon nitride layer to reduce the electrical feed-through as GaN is un-intentionally doped. Silicon nitride layer was subsequently patterned and GaN was plasma etched using BCl_3/Cl_2 (Fig. 3(a)). The top electrode (Ti/Au) and ground pads were deposited and patterned using the lift-off process. An additional 400 nm of gold was deposited and patterned on the ground electrode and the input/output pads to reduce the contact resistance (Fig. 3(b)). The 10 µm thick silicon device layer was then etched around contours of devices with deep reactive ion etching (DRIE) (Fig. 3(c)). The silicon handle layer was etched from the backside. Finally, the buried oxide was plasma etched and devices were released (Fig. 3(d)). Fig. 4 shows a scanning electron microscope (SEM) image of a GaN-on-silicon TPoS filter. The RF measurement results of this filter as well as several other devices are presented in the following sections.

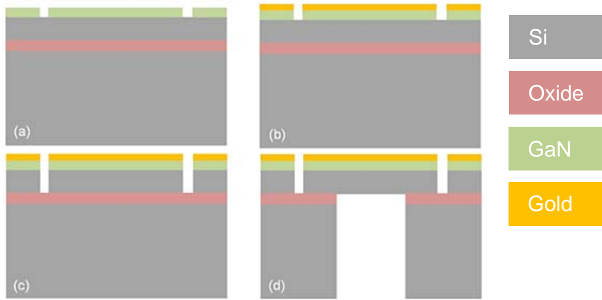

Fig. 3. Fabrication process flow of GaN-on-silicon TPoS filters.

Results

The RF measurements were carried out using a Suss Microtek PM5 Probe station, an Agilent N5241A PNA, and GSG ACP40 probes from Cascasde Microtech. Short-Open-Load-Through (SOLT) calibration was performed prior to measurements. All measurements were taken with 50 Ω termination impedances.

The operating frequency of a TPoS filter is decided by the thickness and material composition of the stack. The device shown in Fig. 4 has its fifth-order thickness resonance mode at 2.1 GHz (Fig. 5). The bandwidth and the loss of the filter are determined by the number of top electrode fingers, electrode geometry, spacing, and active electrode area [11]. The bandwidth of this filter with electrode width of 10 µm and electrode spacing of 3 µm is 20.2 MHz (Fig. 5). COMSOL multi-physics software was used to simulate the frequency response of the device (Fig. 6(a)). The measured response (Fig. 6(b)) agrees reasonably with the simulated response. Knowledge of precise material properties and thickness is necessary for an accurate simulation; uncharacterized AlN/AlGaN layer and fabrication errors can explain the discrepancy between the simulated and measured results.

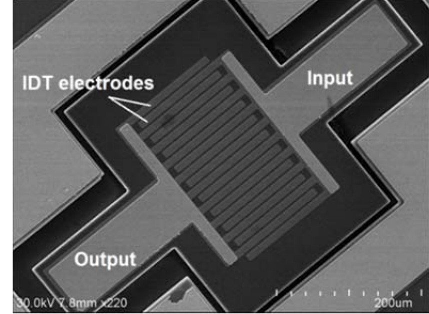

Fig. 4. A SEM image of a GaN-on-silicon filter with electrode width of 10 µm, electrode spacing of 3 µm and active area of 260×240 µm^2.

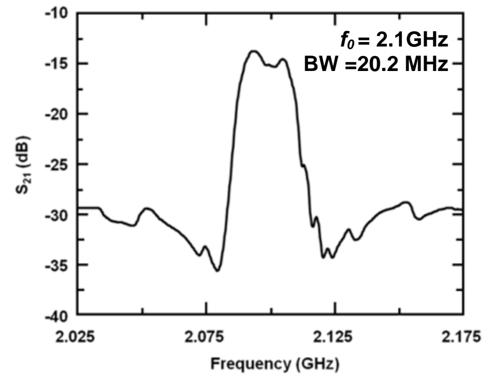

Fig. 5. Measured frequency response of the device shown in Fig. 4.

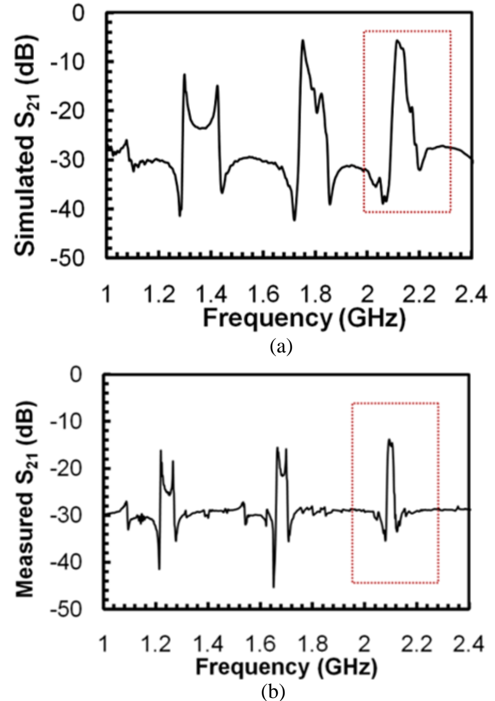

Fig. 6. Wide-band response of the device in Fig. 4, showing a good match between the simulated (a) and measured (b) frequency responses.

The second-order thickness mode of a TPoS filter demonstrates a high Q of 1850 at 802.5 MHz at ambient pressure and room temperature (Fig. 7), which results in the highest $f{\times}Q$ value of $1.5{\times}10^{12}$ reported to date.

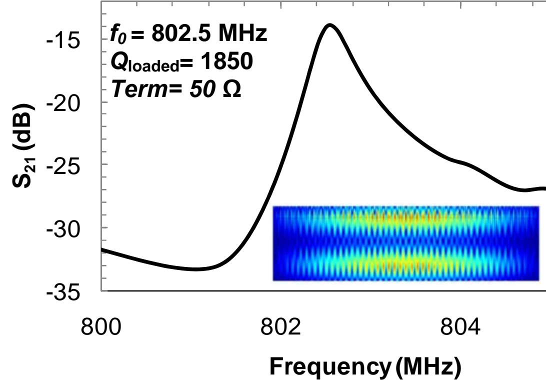

Fig. 7. Measured S_{21} response of a TPoS filter at 802.5 MHz. Inset shows the mode shape obtained using ANSYS.

In addition to TPoS filters, film bulk acoustic resonators (FBARs) have been fabricated on the same substrate. An apodized FBAR shown in Fig. 8 exhibits loaded Q of 210 at its fifth-order thickness-mode resonance frequency of 2.10 GHz (Fig. 9). The unloaded Q of the resonator is extracted to be 424, demonstrating an $f{\times}Q$ value of $0.89{\times}10^{12}$. The extracted k_t^2 of the FBAR shown in Fig. 8 is 1.7% which agrees favorably with the theoretical value of 1.9 % reported in the literature [12].

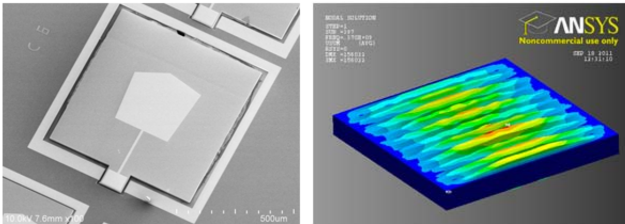

Fig. 8. (left) A SEM image of an apodized GaN-on-silicon FBAR with an active area of 81600 μm^2. (right) ANSYS simulation of the FBAR showing the first-order thickness mode frequency at 370 MHz.

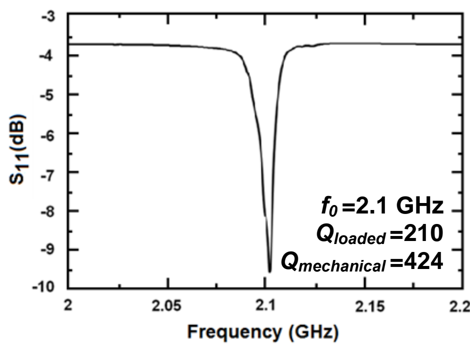

Fig. 9. Measured response of the GaN-on-silicon FBAR shown in Fig. 8. Extracted mechanical Q is 424 at 2.1 GHz.

Mason's model can be used to predict the thickness-mode frequency and the impedance of resonators. The Mason's model [13] translates each layer in the resonator stack to a T-network, based on the material's thickness and acoustic velocity, defined as $Z_{acoustic} = \rho{\times}v$, where ρ is the mass density and v is the acoustic velocity in the material. C_C is the clamped capacitance given by $C_C=A/(\beta^S t)$, where A is the area of the electroded region, t is the thickness of the piezoelectric layer, and β^S is the dielectric impermeability of the piezoelectric material at a constant strain (Fig. 10). Using this model, the fundamental thickness mode frequency, estimated at 365 MHz, and the four overtones of the FBAR in Fig. 8 are depicted (Fig. 11). In Fig. 11, the measured impedance plot of the FBAR is overlapped with the response using the Mason's model showing a good match.

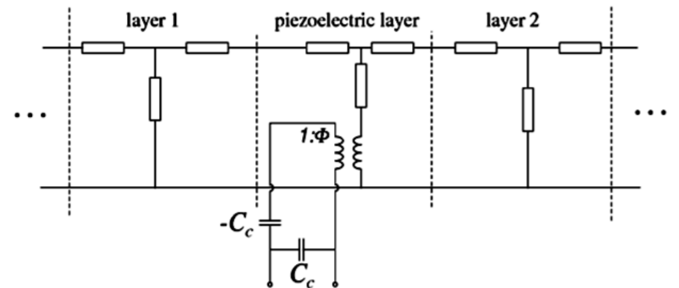

Fig. 10. Mason's model of a thickness-mode resonator.

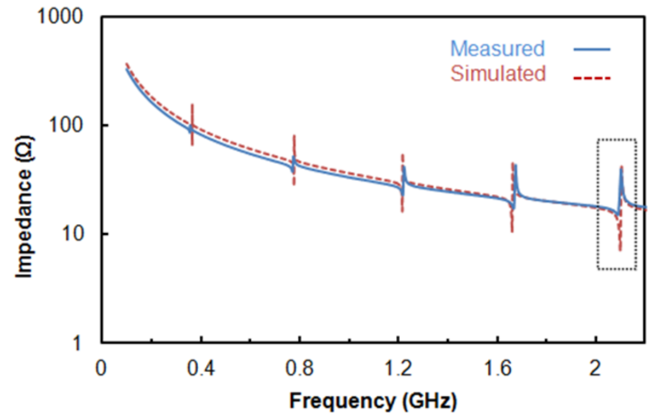

Fig. 11. Simulated and measured impedance plots of the FBAR in Fig. 8 in a wide frequency range, showing a good match between the measured and simulated responses. The impedance is shown in logarithmic scale.

Characterization and Discussion of the Results

A. Power Handling

Nonlinearities of the piezoelectric resonators introduce distortion and noise and therefore limit the output power level. The added silicon in the stack improves the power handling capability as the thick silicon has a higher energy density [6]. The frequency response of the TPoS filter at different power levels clearly shows that the distortion introduced at higher power levels is negligible (Fig. 12).

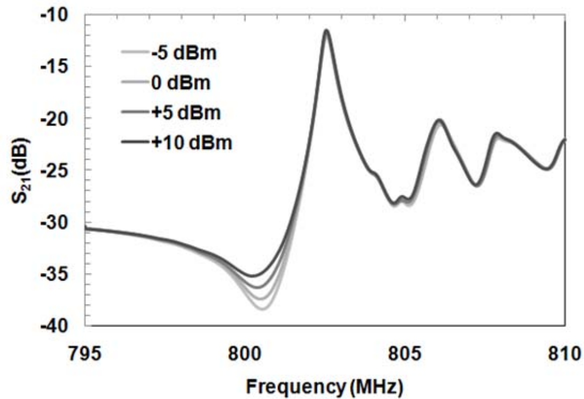

Fig. 12. Measured S_{21} response of the TPoS filter shown in Fig. 4 at different power levels.

B. Temperature Coefficient of Frequency

Fig. 13 shows the variation of resonance frequency over a temperature range of 150 K to 300 K. The frequency drops linearly in this range. The temperature coefficient of frequency (TCF) of the GaN-on-silicon resonator is extracted to be -20.4 ppm/K. As a reference, TCF of unintentionally doped GaN and un-doped silicon are -17.7 ppm/K [2] and -30 ppm/K [14], respectively.

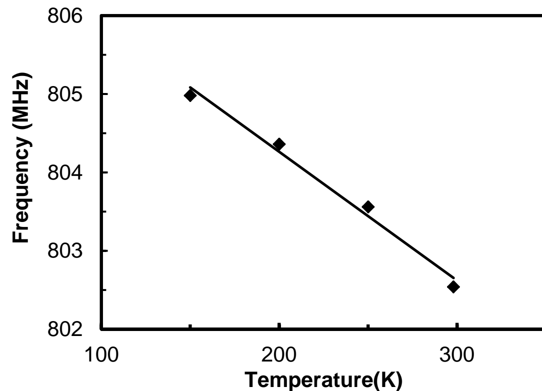

Fig. 13. Linear resonance frequency variation of TPoS filter in Fig. 4 over a temperature range of 150 K to 300 K.

Conclusion

This work presents the first example of fabrication and characterization of resonant micromechanical devices fabricated using GaN-on-silicon. The use of this configuration enables leveraging the excellent acoustic properties of silicon with piezoelectric properties of GaN. This combination has significant advantages over contemporary technologies in terms of performance and integration with silicon electronics. By utilizing this technique, a record Q of 1.5×10^{12}, k_t^2 of 1.7% and high power handling capability is reported. However, as the SEM view in Fig. 14 indicates, the side wall profile is not smooth, showing that the performance of the devices can be considerably improved with an optimized fabrication process.

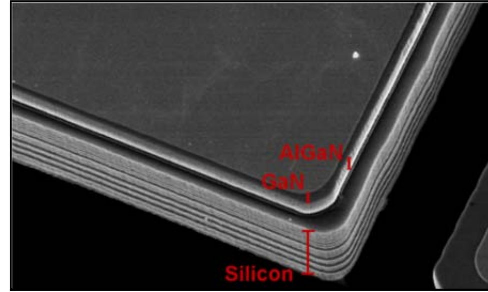

Fig. 14. A SEM image showing the side wall of a GaN-on-silicon resonator.

Acknowledgement

The authors would like to acknowledge the staff of the Lurie Nanofabrication Facility at the University of Michigan for their assistance with fabrication. This work was funded by the U.S. Army Research Laboratory under contract W911NF and prepared through collaborative participation in the MAST CTA and by NSF under award # 1002036.

References

[1] Z. C. Feng, *III-nitride Semiconductor Materials*, Imperial College Press, 2006.

[2] V. J. Gokhale, J. Roberts, and M. Rais-zadeh, "High performance bulk-mode Gallium Nitride resonators and filters," *Transducers*, Beijing, 2011.

[3] V. J. Gokhale, Y. Shim, V. A. Thakar, and M. Rais-Zadeh, "*Q* amplification in Gallium Nitride thickness mode filters using acoustoelectric effect," *Tech. Dig. Solid-State Sensors, Actuators, and Microsystems Workshop*, Hilton Head Island, SC, 2010.

[4] W. Pan, and F. Ayazi, "Thin-film piezoelectric-on substrate resonators with *Q* enhancement and TCF reduction," *IEEE MEMS conference, Tucson, AZ*, 2008.

[5] G. K. Ho, R. Abdolvand, A. Sivapurapu, S. Humad, and F. Ayazi, "Piezoelectric-on-silicon lateral bulk acoustic wave micromechanical resonators," *Journal of MEMS*, vol. 17, no. 2, pp. 512-520, Apr. 2008.

[6] R. Abdolvand, H. M. Lavasani, G. K. Ho, and F. Ayazi, "Thin-film piezoelectric-on-silicon resonators for high-frequency reference oscillator applications," *IEEE Transactions on Ultrasonics, Ferroelectrics, and Frequency Control*, vol. 55, no. 12, pp. 2596-2606, Dec. 2008.

[7] H. Chandrahalim, et al., "Influence of silicon on quality factor, motional impedance and tuning range of PZT transduced resonators," *Hilton Head*, 2008.

[8] A. Muller et al., "6.3-GHz film bulk acoustic resonator structures based on a GaN/Silicon thin membrane," *IEEE Electron Device Letters*, Vol.30, No.8, pp.799-801, Aug. 2009.

[9] K. Brueckner et al., "Two-dimensional electron gas based actuation of piezoelectric AlGaN/GaN microelectromechanical resonators," *Applied Physics Letters*, vol. 93, no.17, p. 173504, Oct. 2008.

[10] J. Cao, D. Pavlidis, Y. Park, J. Singh, and A. Eisenbach, "Improved quality GaN by growth on compliant silicon-on-insulator substrates using metalorganic chemical vapor deposition," *Journal of Applied Physics*, vol. 83, no. 7, Apr. 1998.

[11] R. F. Milson, D.T. Elliot, S. Terrywood, and M. Redwood, "Analysis and design of coupled-mode miniature bar resonators and monolithic filters," *IEEE Transactions on Sonics and Ultrasonics,* vol. 30, no. 3, May 1983.

[12] D. Neculoiu et al., "Microwave FBAR structures fabricated using micromachined GaN membranes," *International Microwave Symposium, IEEE/MTT-S*, pp. 877–880, June 2007.

[13] W. P. Mason, *Electromechanical Transducers and Wave Filters*, Van Nostrand Co., New York, 1948.

[14] S. Pourkamali, G. K. Ho, and F. Ayazi, "Low-Impedance VHF and UHF Capacitive SiBARs, Part I," *IEEE Transaction on Electron Devices,* vol. 54, no. 8, pp. 2017-2023, Aug. 2007.